Science of the Total Environment 409 (2011) 2917–2928

Contents lists available at ScienceDirect

Science of the Total Environment

journal homepage: www.elsevier.com/locate/scitotenv

Wavelet and ANN combination model for prediction of daily suspended sediment load in rivers

Taher Rajaee

Department of Civil Eng., University of Qom, Qom, Iran

ARTICLE INFO

Article history:
Received 19 August 2009
Received in revised form 19 November 2010
Accepted 23 November 2010
Available online 4 May 2011

Keywords:
Artificial neural network
Wavelet analysis
Suspended sediment load
Hysteresis
Yadkin River
Multi linear regression

ABSTRACT

In this research, a new wavelet artificial neural network (WANN) model was proposed for daily suspended sediment load (SSL) prediction in rivers. In the developed model, wavelet analysis was linked to an artificial neural network (ANN). For this purpose, daily observed time series of river discharge (Q) and SSL in Yadkin River at Yadkin College, NC station in the USA were decomposed to some sub-time series at different levels by wavelet analysis. Then, these sub-time series were imposed to the ANN technique for SSL time series modeling. To evaluate the model accuracy, the proposed model was compared with ANN, multi linear regression (MLR), and conventional sediment rating curve (SRC) models. The comparison of prediction accuracy of the models illustrated that the WANN was the most accurate model in SSL prediction. Results presented that the WANN model could satisfactorily simulate hysteresis phenomenon, acceptably estimate cumulative SSL, and reasonably predict high SSL values.

1. Introduction

The modeling and prediction of river suspended sediment are key elements in the global water recourses and environment policy and management. The prediction of SSL which is a nonlinear and complex phenomenon is not a simple task. In the past decades, numerous studies have been conducted in the modeling of sediment processes. Commonly, mathematical models are employed for this object (Verstraeten and Poesen, 2001; Ward et al., 2009); which these techniques usually need a lot of data and a long response time. Studies have been conducted to reduce the complexities of the problem in terms of developing practical techniques that do not require dwell on algorithm and theory. In this way classic models such as MLR and SRCs are widely used for suspended sediment modeling (Kisi, 2005). However, they are basically linear models assuming that data are stationary, and have a limited ability to capture non-stationarities and non-linearities in hydrological and environmental data. In recent years, the use of artificial intelligence approaches is increasing due to their capability. In the field of water resources and environmental engineering, ANN models have recently been applied to pesticide contamination modeling in shallow groundwater (Sahoo et al., 2006), simulation of polluted stream (Kim et al., 2008), estimation of scour depth near pile groups (Zounemat-Kermani et al., 2009), and forecasting of ozone episode days (Tsai et al., 2009).

On behalf of river sediment prediction, using artificial intelligence approaches, ANN employment has been studied recently (Nagy et al., 2002; Bhattacharya et al., 2005; Raghuwanshi et al., 2006; Zhu et al., 2007; Alp and Cigizoglu, 2007). The characteristics of these researches are presented in Table 1. Nagy et al. (2002) developed an ANN model to estimate suspended sediment concentration (SSC) in rivers, achieved by training the ANN model to extrapolate several stream data collected from reliable sources. The network was set up using several parameters, such as Froude number, stream width ratio, mobility number and Reynolds number, as the input pattern and the SSC as the output pattern. A comparison among the ANN model and several commonly used sediment discharge formulas was performed on 80 data observations. A discrepancy ratio $D_r = C_c/C_m$ was used for comparison, where C_c is the calculated and C_m is the measured total load concentration. In model testing, ANN's results are better than other commonly used sediment discharge formulas. The discrepancy ratio for ANN was 1.04, where as this parameter was 2.34 and 0.41 for Engelund and Hansen (1967) and Toffaleti (1969) formulas, respectively. Bhattacharya et al. (2005) provided an algorithm for developing a data-driven method to forecast sediment transport (total) rates using ANN. Published flume and field data from several researchers have been employed to build the ANN model. The predictive accuracy of the model was found to be better than well-known sediment transport models such as Engelund and Hansen. Raghuwanshi et al. (2006) proposed an ANN model to runoff and sediment yield modeling in Nagwan watershed in India. A five-year data set was employed for training and a two-year data set was considered for testing the model. Linear regression based daily and weekly runoff and sediment yield prediction models were also developed using the above training data set and were tested using the testing data set. The ANN models performed better than the linear regression models in

E-mail addresses: trajaee@qom.ac.ir, taher_rajaee@yahoo.com.

0048-9697/$ – see front matter
doi:10.1016/j.scitotenv.2010.11.028

Table 1
Some illustrative reviews of ANN applications in sediment modeling.

Authors	Temporal scale	Case study	Time period	Independent variables	Dependent variable
Nagy et al., 2002		Niobrara River, Middle Loup River, Hii River, Rio Grande River, Mississippi River and Sacramento River	Experimental data	Froude number, stream width ratio, Reynolds number, shear velocity and the depth ratio	Total load concentration (ppm)
Bhattacharya et al., 2005		55 flume and 24 field datasets	Experimental data	Water depth, flow velocity, particle size and energy slope	Dimensionless total transport rate
Raghuwanshi et al., 2006	Daily and weekly	Nagwan watershed, Hazaribagh, Jharkhand, India	(June to October), data from 1991–1997	Rainfall and temperature	Runoff (mm) and sediment yield (ton/ha)
Zhu et al., 2007	Monthly	Longchuanjiang River, the Upper Yangtze Catchment, China	1960 to 2001	Average rainfall, temperature, rainfall intensity and water discharge	Suspended sediment flux (kg/s)
Alp and Cigizoglu, 2007	Daily	Juniata River, Pennsylvania, USA	1 January 1983 to 7 June 1989	Rainfall flow and SSL	SSL (ton/day)
Rajaee et al., 2009	Daily	Little Black River (LBR) and Salt River (SR) stations, Missouri State, USA	October 1, 1980 to September 30, 1984 (in LBR) October 1, 1984 to September 30, 1988 (in SR)	River discharge and SSC	SSC (mg/l)
Rajaee, 2010	Daily	Potomac River at Point of Rocks, MD gauging station, USA	October 1, 1960 to September 30, 1989	River discharge and SSL	SSL (ton/day)

predicting both runoff and sediment yield on a daily and weekly simulation scale. Zhu et al. (2007) proposed an ANN model for simulating the monthly suspended sediment flux in the Longchuanjiang River in China. In the mentioned model, suspended sediment flux was related to the average rainfall, temperature, rainfall intensity, and flow discharge. Results illustrated that the ANN model is capable of simulating monthly suspended sediment flux with fairly good accuracy concerning proper variables and their correlation to the previous month (lagging effect) on the suspended sediment flux. In the research performed by Alp and Cigizoglu (2007), the relation between hydrometeorological variables (rainfall and flow) and total daily suspended sediment load was evaluated using two ANN methods; feed forward back propagation and radial basis function techniques. The ANNs were trained using rainfall flow and suspended sediment load data from the Juniata catchment in the USA. The ANN models provided satisfying results in terms of the selected performance criteria comparing with conventional multi linear regression. Rajaee et al. (2009) studied ANN, MLR, and SRC models for daily simulation of SSC in two hydrometry stations. The models were trained using daily river discharge and SSC data belonging to Little Black River and Salt River gauging stations in the USA. Comparison of the models' results indicated that the ANN model had more ability in predicting SSC in comparison with the MLR and SRC models. Furthermore, the results indicated that the ANN model could reasonably estimate cumulative SSL and acceptably simulate hysteresis phenomenon. In another study, Rajaee (2010) proposed a model by combining the wavelet analysis and neuro-fuzzy (NF) approach to predict daily suspended sediment in a gauging station in the USA. In the developed model, daily observed time series of river discharge and suspended sediment were decomposed to some sub-time series. Obtained results showed that the proposed model performs better than the NF and SRC models in prediction of suspended sediment.

Wavelet analysis, which provides information in both the time and frequency domains of the signal, gives considerable insight into the physical form of the data. Wavelet analysis has been applied to a number of problems in water resources and environmental engineering, including rainfall–runoff modeling in a karstic watershed (Labat et al., 1999), river flow modeling (Pasquini and Depetris, 2007), meteorological pollution simulation (Osowski and Garanty, 2007), characterization of daily stream flow (Saco and Kumar, 2000), and open channel wake flows analysis (Addison et al., 2001). It has been found that an appropriate data pre-processing which employs wavelet analysis can lead to models that more sufficiently represent the true characteristics of the underlying system.

ANN and wavelet analysis are presented to be successful when they are applied individually to water resources and environmental problems. Recently, there has been a growing interest in combined methods. Some research has proposed hybrid wavelet–ANN models. Kim and Valdes (2003) provided a wavelet–ANN model to predict droughts in Mexico. Cannas et al. (2005) proposed a hybrid wavelet–ANN model for monthly rainfall–runoff modeling in Italy and Tantanee et al. (2005) proposed a coupled wavelet-autoregressive model for annual rainfall prediction. Cannas et al. (2006) studied the effects of data pre-processing on the ANN model performance using continuous and discrete wavelet transforms. Each of these researches showed that the ANNs calibrated with the pre-processed data resulted in better efficiency in comparison to the ANNs which were calibrated with un-decomposed, noisy raw time series.

According to the previously mentioned qualitative analysis, a hybrid model for suspended sediment prediction based on wavelet analysis and ANN is proposed and discussed in this research. The goal of combining the wavelet analysis and ANN model is improving the accuracy of SSL prediction. Therefore, a WANN model which uses multi-scale signals as input data may present more reliable predictions rather than a single pattern input.

The current research is a new application of the wavelet–ANN hybrid model, which uses multi-scale signal, for prediction of SSL. The rest of the paper is organized as following; hydrometry station and statistical analysis are presented in Section 2. In Section 3, ANNs, wavelet transform, MLR, SRC, and proposed WANN models are described. The model application for a real world problem and results are summarized at Sections 4 and 5. The summary and conclusion will be the last section.

2. Hydrometry station and statistical analysis

2.1. Hydrometry station

The data obtained from the Yadkin River at Yadkin College, NC gauging station (USGS Station No: 02116500, Basin Area (sq. mi.): 2280, longitude: 080°23′10″ and latitude: 35°51′24″) in Virginia State, operated by the U.S. Geological survey (USGS), were employed to train and test all the models developed in this paper. Fig. 1 shows the Yadkin River and the gauging station.

The data from October 1, 1957 to September 30, 1982 (25 years; i.e. 83% of total data) and the data from October 1, 1982 to September 30, 1987 (5 years; i.e. 17% of total data) were used for training and testing sets, respectively. Daily time series of Q and SSL were downloaded from the web server of the USGS (http://co.water.usgs.

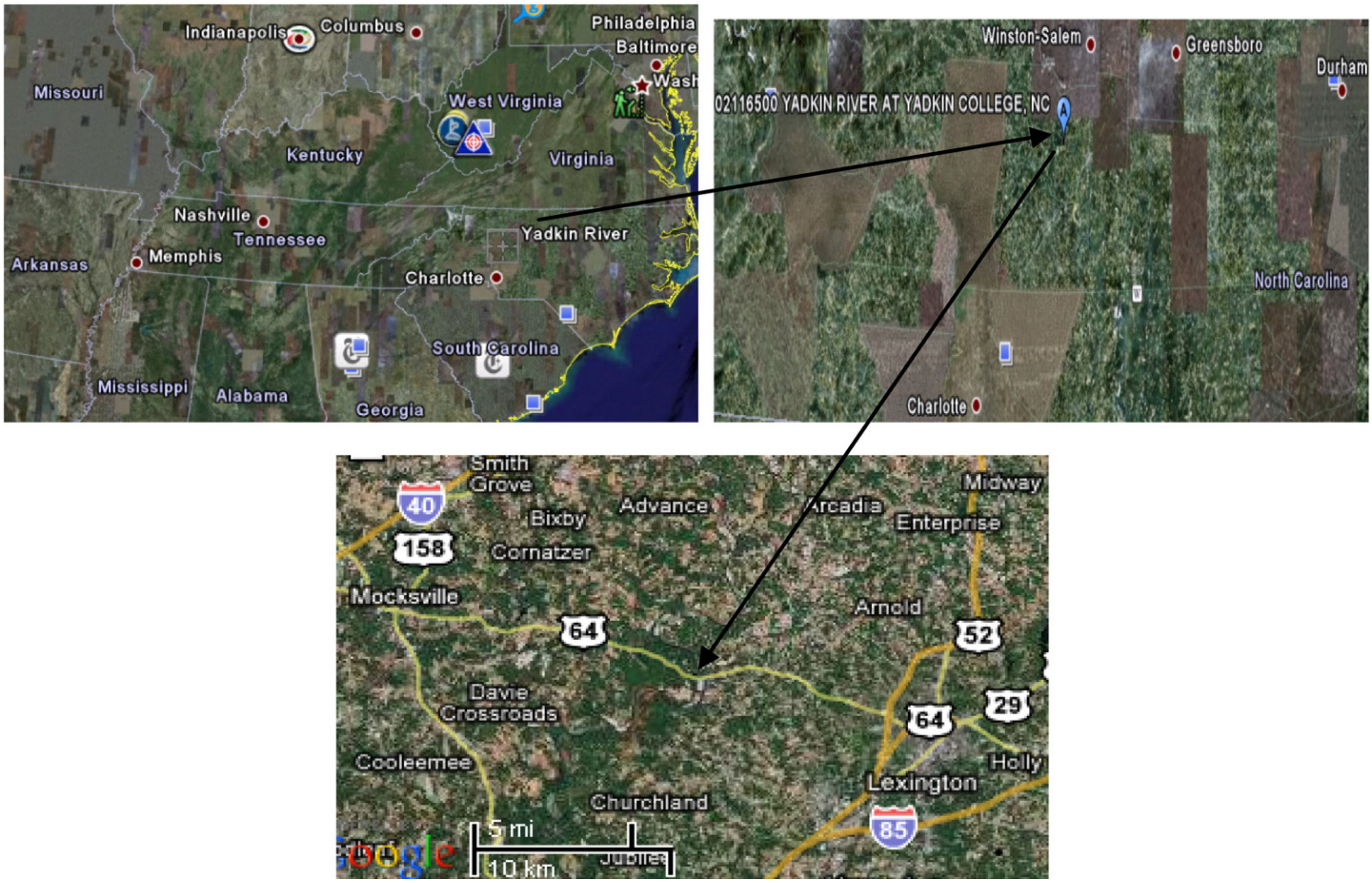

Fig. 1. Yadkin River at Yadkin College, NC.

gov/sediment/seddatabase.cfm). Fig. 2 shows these time series of data related to daily Q and SSL.

The consideration of the first 25 years of the Q and SSL time series for the calibration set has two advantages; first, the highest observed Q and SSL occurred during this period and second, considering significant variations could be possible.

2.2. Statistical analysis

The statistical analysis for training and testing sets is given in Table 2, which contains the minimum, maximum, standard deviation (S_d), mean, skewness coefficient (C_{sx}), lag 1 day autocorrelation coefficient(R_1), lag 2 days autocorrelation coefficient (R_2), lag 3 days autocorrelation coefficient (R_3), and lag 4 days autocorrelation coefficient (R_4).

It should be noted that, similar to all empirical models, ANN models perform best when they do not extrapolate beyond the range of the data used for model training (Tokar and Johnson, 1999). From Table 2, it could be observed that the extreme values of Q and SSL were in the training set. When dividing the data into training and testing subsets, it is essential to check the data which present the same statistical population (Masters, 1993). In general, Table 2 illustrated relatively similar statistical characteristics between training and testing sets in terms of mean, standard deviation, skewness coefficient, and autocorrelation coefficients. River discharge autocorrelation coefficients, especially R_1, were high, but SSL autocorrelation coefficients, except for R_1, were very low in both training and testing data sets. Skewness coefficients were low for both training and testing sets. This is appropriate for modeling, because high skewness coefficient has a considerable negative effect on ANN performance (Altun et al., 2007). The correlation coefficients between observed

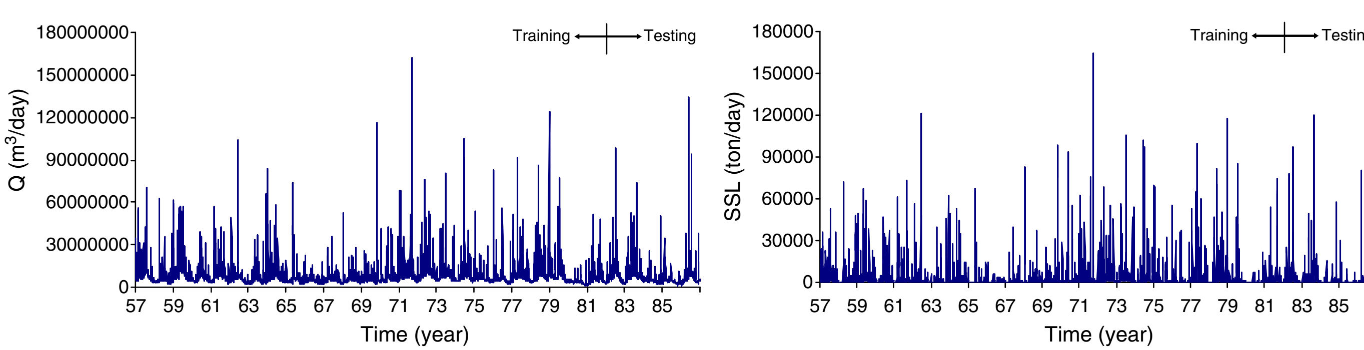

Fig. 2. River discharge and SSL time series (30 years).

Table 2
Statistics analysis for training, testing and all data sets.

Statistical parameters	All data		Training set		Testing set	
	Q (m^3/day)	SSL (ton/day)	Q (m^3/day)	SSL (ton/day)	Q (m^3/day)	SSL (ton/day)
Mean	7.68×10^6	2246.7	7.76×10^6	2345.9	7.26×10^6	1751
S_d	7.79×10^6	7324	7.76×10^6	7360.7	7.93×10^6	7118.9
C_{sx}	6.15	8.21	6.01	7.93	6.85	9.82
Min	889,920	8.23	889,920	8.23	1,166,400	13.03
Max	161,568,000	1.648×10^5	161,568,000	1.648×10^5	133,920,000	1.206×10^5
R_1	0.737	0.521	0.733	0.531	0.752	0.465
R_2	0.437	0.189	0.43	0.2	0.468	0.125
R_3	0.323	0.111	0.317	0.118	0.35	0.068
R_4	0.276	0.082	0.272	0.087	0.295	0.047

SSL_t and Q time series are calculated in order to obtain suitable input pattern for ANN, WANN, and MLR models. The results are shown in Table 3. The correlation coefficient (ρ) between Q and SSL, which for n pairs are available, is defined as:

$$\rho = \frac{\sum_{i=1}^{n}\left(Q_i-\bar{Q}\right)\left(SSL_i-\bar{SSL}\right)}{\sqrt{\sum_{i=1}^{n}\left(Q_i-\bar{Q}\right)^2\sum_{i=1}^{n}\left(SSL_i-\bar{SSL}\right)^2}} \tag{1}$$

where the bar denotes the mean of the variable.

The higher values of correlation coefficient, which range from 0 to 1, indicate better agreement between the variables. To make a suitable selection of model input variables, the autocorrelation and cross-correlation between the Q and SSL data were investigated. This technique was acceptably used by Fernando and Kerr (2003). As can be seen from Table 3, the correlation between SSL_t and Q_{t-1} and also the correlation between SSL_t and Q_{t-2} are relatively high; therefore, SSL was related to the Q_{t-1} and Q_{t-2} in the models.

It is common to use a linear method for normalization of data; therefore, in this study the data are pre-processed by scaling them between 0 and 1 to eliminate their dimension and to ensure that all variables are equally given attention during calibrating and testing of the models. The following simple linear mapping of the variables is the most common technique for this purpose. For SSL variable with minimum and maximum values of $SSL_{\min}$ and $SSL_{\max}$, respectively, the scaled value SSL_n is computed as the following:

$$SSL_n = \frac{(SSL-SSL_{\ min})}{(SSL_{\ max}-SSL_{\ min})}. \tag{2}$$

3. Methods

3.1. Artificial neural networks

In the last two decades, the ANN approach has received a great deal of attention as a tool of computation by many researchers. The first fundamental concepts related to neural computing were developed by McCulloch and Pitts (1943) and much of the ANN activities have been centered on back-propagation and its extensions (Salas et al., 2000). ANN, a massively parallel distributed information processing system, is based on concepts derived from research on the nature of human brains (Muller et al., 1995). A common three-layered feed-forward neural network comprised multiple elements, called nodes, and connection pathways that links them (Haykin, 1999). The nodes are processing elements of the network and are normally known as neurons. The neurons having similar properties are grouped in one single layer. These networks are made up of an input layer consisting of nodes representing different input variables, the hidden layer consisting of many hidden nodes and an output layer consisting of output variables. In the hidden and output layers, the net input to unit i is:

$$y_i = \sum_{j=1}^{p} w_{ij}x_j + \theta_i \tag{3}$$

where $w_{ji}=(w_1,w_2,...,w_{pi})$ is the weight vector of unit i and p is the number of neurons in the above layer of unit i, x_i is the output from unit j and θ_i is the bias of unit i. This weighted sum y_i; which is called the incoming signal of unit i, is then passed through a transfer function. A recommended literature for the ANN approach could be Masters (1993).

3.2. Wavelet analysis

Wavelet approach is a time-dependent spectral analysis that decomposes time-series in the time–frequency space to provide a timescale illustration of processes and their relationships (Daubechies, 1990). Wavelet transform (WT) is a successful technique to capture the characteristics of target time series and to detect localized phenomena in nonstationary time series. This method is a powerful signal processing tool used in a time series analysis. The WT is similar to the Fourier transform, in the sense that a time series is presented as a linear combination of some base functions. For the WT, the base functions are translations and dilations of one function called the mother wavelet.

The current study will not delve into the theory behind wavelet transform and only the main concepts of the discrete wavelet transform (DWT) are briefly presented. A mathematical overview of WT and a review of applications is presented by Labat et al. (2000). The WT performs the decomposition of a signal into a group of functions (Cohen and Kovacevic, 1996):

$$\psi_{j,k}(x) = 2^{j/2}\psi_{j,k}\left(2^jx-k\right) \tag{4}$$

where $\psi_{j,k}(x)$ is produced from a mother wavelet $\psi(x)$ which is dilated by j and translated by k. The mother wavelet has to satisfy the condition.

$$\int\psi(x)dx = 0 \tag{5}$$

Table 3
The correlation coefficients between measured SSL_t and Q.

Time series	All data	Training set	Testing set
Q_t	0.862	0.868	0.829
Q_{t-1}	0.451	0.46	0.402
Q_{t-2}	0.199	0.205	0.162
Q_{t-3}	0.134	0.138	0.109
Q_{t-4}	0.114	0.117	0.096

The discrete wavelet function of a signal $f(x)$ can be calculated as follows:

$$c_{j,k} = \int_{-\infty}^{\infty} f(x)\psi_{j,k}^{*}(x)dx \tag{6}$$

$$f(x) = \sum_{j,k} c_{j,k}\psi_{j,k}(x) \tag{7}$$

where $c_{j,k}$ is the approximate coefficient of a signal. The mother wavelet is formulated from the scaling function $\varphi(x)$ as:

$$\varphi(x) = \sqrt{2}\sum h_0(n)\varphi(2x-n) \tag{8}$$

$$\psi(x) = \sqrt{2}\sum h_1(n)\varphi(2x-n) \tag{9}$$

where $h_1(n)=(-1)^n h_0(1-n)$. Different sets of coefficients $h_0(n)$ can be found corresponding to wavelet bases with various characteristics. In the DWT, coefficients $h_0(n)$ play a critical role (Gupta and Gupta, 2007).

3.3. Multi linear regression (MLR) analysis

MLR is a technique used to model the linear relationship among a dependent variable and one or more independent variables. The common form of MLR is described as:

$$Z = a_0 + \sum a_i Y_i \tag{10}$$

where a_0 is the intercept, a_i is the regression coefficient of the descriptor Y_i, and Z is the predicted value. Determination of the values of the parameters of the regression equation is the goal of the MLR method. The MLR method is based on some assumptions. The regression estimators are optimal in the sense that they are unbiased, efficient, and consistent. Unbiased means that the expected value of the estimator is equal to the accurate value of the parameter. Efficient means that the estimator has a smaller variance than any other estimator and consistent means that the bias and variance of the estimator technique zero as the sample size approach infinity. More detailed information for the MLR approach can be found in standard references, such as Snedecor and Cochran (1981).

3.4. Sediment rating curve (SRC) method

A considerable part of sediment in rivers is transported as suspension load. Most of this load consists of silt and clay, i.e. wash load. Thus it can be concluded that wash load plays an important role in the sediment transport in rivers (Asselman, 2000). As the finest fraction of the SSL often is a non-capacity load, it cannot be predicted using stream power related sediment transport models. Instead, empirical relations such as SRCs often are applied (Asselman, 2000). The establishment of a SRC is an important problem in hydrology. The most common SRC is a power function (Walling, 1978). This relation is developed by fitting a power curve between the river discharge and SSL measured data. Commonly the SRC has the form $SSL = aQ^b$, where a and b are constants. In the past decades, inspection was employed to draw a curve on a graph. Recently, regression technique is usually performed to determine parameters a and b.

There are several techniques for estimating SSL from Q in the lack of measured SSL data (Horowitz, 2003). These techniques contain interpolation and extrapolation with potential additional modifications using different correction factors (Holtschlag, 2001). Nevertheless, the basis for the most commonly employed procedure (extrapolation) is the determination of a log–log regression, which relates SSL to Q. The efficiency of this method is dependent on the number of paired data points used to develop the SRC. How well the data present the ranges of Q and SSL at a gauging station is important too (Roberts, 1997).

3.5. Proposed wavelet-artificial neural network (WANN) combination model

In this study, the wavelet transform was linked to the ANN method for prediction of SSL in one day ahead. The wavelet transform technique was employed for time series analysis. The supplementary information was used to display how the SSL periodic time series varies as a function of time. The proposed WANN model for the prediction of SSL is shown in Fig. 3.

To develop the WANN model, firstly measured Q and SSL time series were decomposed to some multi-frequently time series $Q_{d1}(t)$, $Q_{d2}(t)$,...,$Q_{di}(t)$, $Q_a(t)$ and $SSL_{d1}(t)$,$SSL_{d2}(t)$,...,$SSL_{di}(t)$, $SSL_a(t)$ by discrete wavelet transform, which $Q_{d1}(t)$,$Q_{d2}(t)$,...,$Q_{di}(t)$ and $Q_a(t)$ are the details and approximation river discharge time series, respectively; $SSL_{d1}(t)$,$SSL_{d2}(t)$,...,$SSL_{di}(t)$ and $SSL_a(t)$ are the details and approximation SSL time series, respectively; di shows the decomposed time series in ith level and a denotes approximate time series. Then, decomposed Q and SSL time series at different scales were imposed to the ANN method for predicting SSL in one day ahead.

The observed Q and SSL time series were decomposed using mother wavelets in different levels, from 1 to 5 (i.e. into 5 wavelet decomposition levels). For example, the level 3 decomposition of the SSL signal which yields 4 sub-signals (approximation at level 3 and detail at levels 1, 2, and 3) by Daubechies-2 (db2) wavelet are presented in Fig. 4. In Fig. 4, SDW 1 is a SSL discrete wavelet at level 1, SDW 2 is a SSL discrete wavelet at level 2, SDW 3 is a SSL discrete wavelet at level 3, and SDW App. is a SSL discrete wavelet approximation mode.

4. Model application

4.1. Model evaluation

It was indicated that the correlation coefficient (ρ) is unsuitable for model evaluation (Legates and McCabe; 1999). Such researches proposed that a perfect evaluation of model performance should include at least one 'goodness-of-fit' or relative error measure (e.g. coefficient of determination (R^2)) and at least one absolute error measure (e.g. root mean square error (RMSE) or mean absolute error (MAE)). In this paper, the ANN, WANN, MLR, and SRC performances were evaluated using R^2, MAE, and RMSE. In brief, the models' predictions are optimum if R^2, MAE, and RMSE are found to be close to 1, 0, and 0, respectively. The R^2, MAE, and RMSE performance evaluation criteria employed in this paper can be computed utilizing the following equations:

$$R^2 = 1 - \frac{\sum_{i=1}^{n}\left(SSL_{i(measured)} - SSL_{i(predicted)}\right)^2}{\sum_{i=1}^{n}\left(SSL_{i(measured)} - SSL_{i(mean)}\right)^2} \tag{11}$$

$$MAE = \frac{\sum_{i=1}^{n}\left|SSL_{i(measured)} - SSL_{i(predicted)}\right|}{n} \tag{12}$$

$$RMSE = \sqrt{\frac{\sum_{i=1}^{n}\left(SSL_{i(\mathrm{measured})} - SSL_{i(predicted)}\right)^2}{n}} \tag{13}$$

in which n is the number of data points.

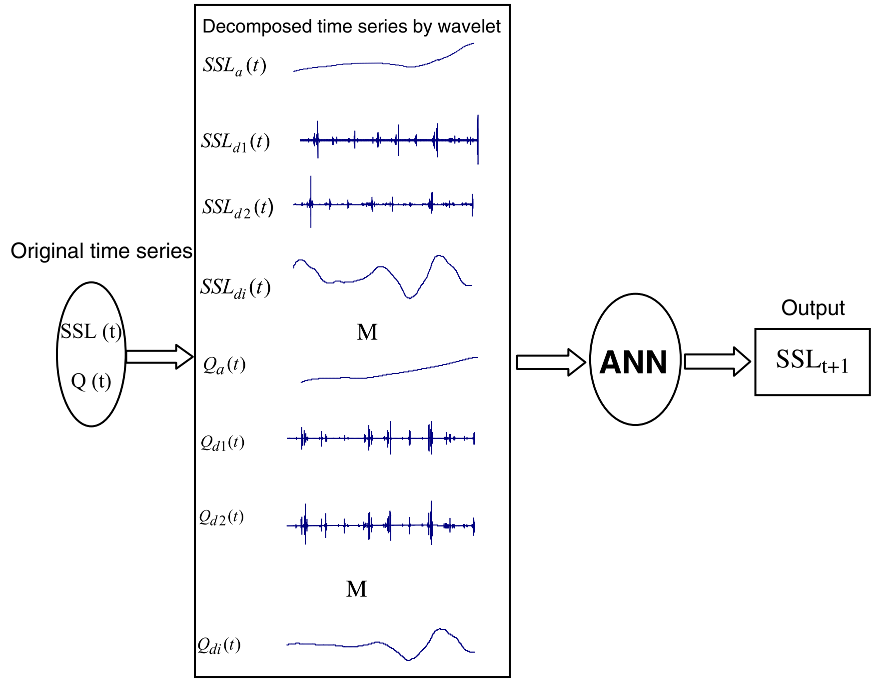

Fig. 3. Structure of the proposed WANN combination model.

4.2. Application of ANN and WANN models

A three layer feed forward neural network (FFNN) with back-propagation (BP) algorithm (Masters, 1993; Haykin, 1999) which contains one input layer, one hidden layer, and one output layer was applied in this research. The standard multilayer FFNN with just one hidden layer using arbitrary squashing functions is capable of approximating any function from one finite dimensional space to another in any desired degree of accuracy, provided sufficiently many hidden units are available. In this sense, multilayer FFNNs are a class of universal approximators (Hornik et al., 1989). The BP algorithm is a gradient descent procedure employed to minimize a least-square objective function (error function). The Levenberg–Marquardt algorithm (Haykin, 1999) was employed to train ANN models. Considering the statistical analysis in Tables 2 and 3, the following combinations that include different values of SSL and Q are considered in the input layer to predict the single SSL in one day ahead at time $t+1$ (SSL_{t+1}) in the output layer in the ANN model.

1) SSL_t
2) SSL_t, SSL_{t-1}
3) SSL_t, SSL_{t-1}, SSL_{t-2}
4) SSL_t, Q_t
5) SSL_t, SSL_{t-1}, Q_t
6) SSL_t, SSL_{t-1}, Q_t, Q_{t-1}

In ANN models, one of the important issues is the type of selected activation function for nodes. The activation function is usually a bounded, continuous, and nonconstant function. The most frequently

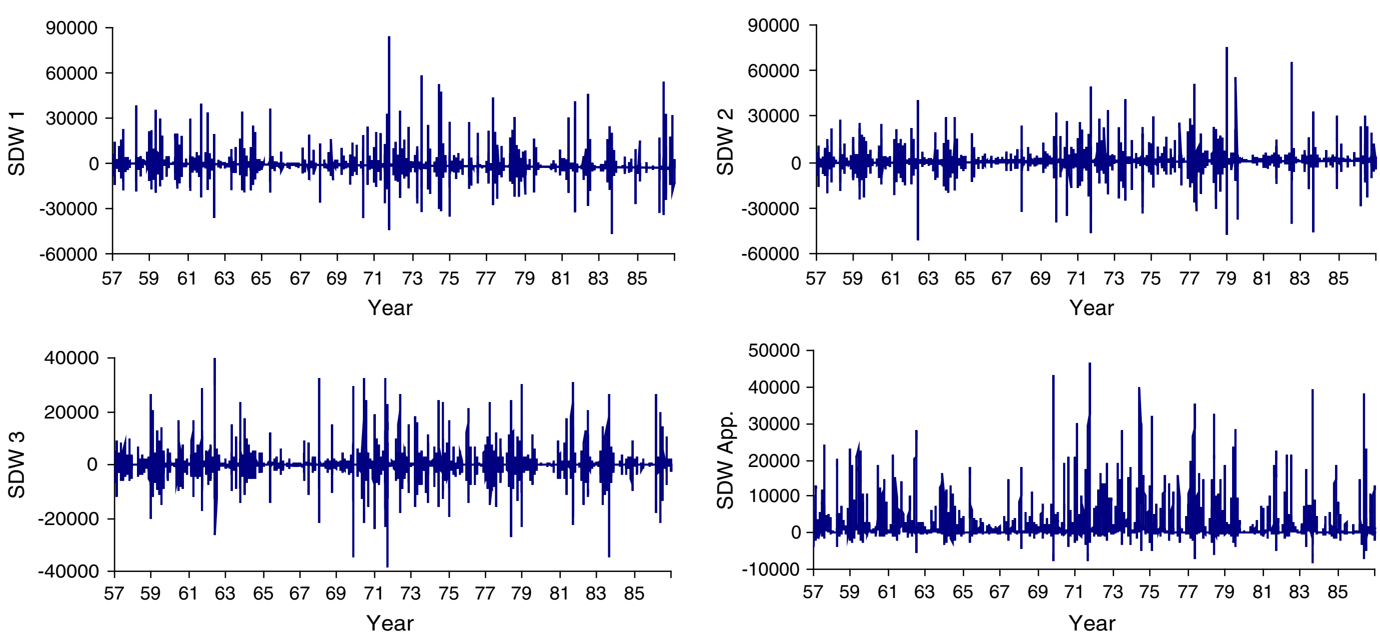

Fig. 4. Detail sub-signals and approximation of db2 (level 3).

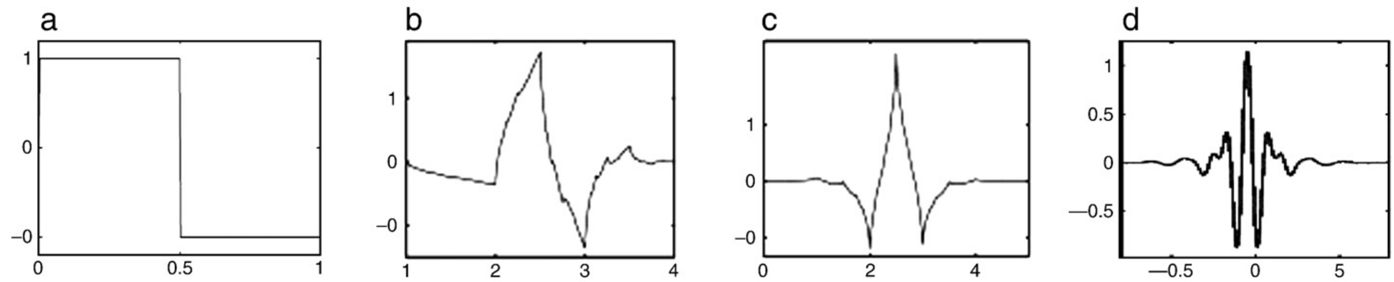

Fig. 5. a) Haar wavelet. b) Db2 wavelet. c) Coif1 wavelet. d) Meyer wavelet.

employed function is the Sigmoid function. This function is differentiable, continuous, and monotonically increasing in its domain. The Sigmoid and Tansig (Schmitz et al., 2006) functions were used as activation functions in hidden and output layers' nodes to make an ANN model more effective. The application of ANN for predicting SSL consists of two steps. The first step is training ANN models and the second one is testing the models. In ANN modeling, two important items should be considered: the ANN structure and the training iteration number (epoch). Appropriate selection of two mentioned items, can progress the model efficiency in both steps of calibration and verification. In addition, it prevents the ANN model to be over trained. In this research, it was concluded that 400 epochs satisfy training network considering 10^{-5} as goal performance. In ANN models, another critical point is determining the number of neurons in input and hidden layers, which provides the best training results. However, there is no specific algorithm to determine the number of required neurons in hidden layer for simulating functions. The number of neurons in the hidden layer, with variation between 2 and 16 was investigated for each input combinations (1–6). Once the training stage was completed, the testing stage begins using the optimum values found for the number of neurons in each input layer and hidden layer. The optimum learning rate, η, and the momentum, α, were obtained after trying different values and observing the RMSE produced at the end of the verification step. It was observed that picking high values like 0.6 and 0.9 for η and α, respectively, as done by Raman and Sunilkumar (1995), throws the network into oscillations or saturates the node outputs. In this paper, it was found that 0.2 and 0.1 are adequate values for η and α, respectively.

In the WANN model, the decomposed SSL and Q time series were entered to the ANN method for prediction of SSL in one day ahead (Fig. 3). For this purpose the dyadic discrete wavelet transforms were used (Mallat, 1989). The number of nodes in the input layer is determined with $(i+1)\times 2$; because the WANN combination model uses two variables (SSL and Q) and each time series is decomposed into i, $i=(1,2,...,5)$ details time series and one approximation time series.

The WANN model employs discrete wavelet transform to overcome the difficulties associated with the conventional ANN model. The wavelet technique can divide the SSL time series properties into various scales of wavelet transform at the same time. Correlation analysis (that is considered in ANN model inputs) provides information on the global functioning of SSL time series, but cannot take the temporal variability of the time series into account, which often leads to a nonlinear and non-stationary functioning of the presses. So, the wavelet approach was presented to focus on the non-stationary properties of time series. The unknown periodical characteristics of SSL time series could be detected using the WANN model.

An important step of wavelet analysis is to select an appropriate wavelet function called “mother wavelet” and then perform analysis using shifted and dilated version of this wavelet. In this study, it was intended to investigate the effects of the employed wavelet type as well as decomposition level on the WANN model efficiency. To achieve this purpose, the SSL and Q time series were decomposed to 1, 2, 3, 4, and 5 levels by seven different kinds of wavelet transforms, i.e. Haar wavelet (a simple wavelet), Daubechies-2 (db2) wavelet (a most popular wavelet) (Mallat, 1989), and some irregular wavelets such as sym1, bior1.1, rboi1.1, Meyer, and coif1 wavelet. For instance, Haar, db2, coif1, and Meyer wavelets are shown in Fig. 5. In this study not only the sensitivity of the pre-processing to the wavelet type and decomposition level is investigated but also the effect of number of inputs is examined as a multivariate simulation.

In the case that the accuracy of the different kinds of wavelet transforms is sufficient, all periodical properties of SSL time series and their role in the SSL phenomenon will be considered in the WANN model.

4.3. Application of MLR and SRC models

MLR and SRC methods were employed to model the relationship between the input variables and the SSL. Six MLR models with the same input combinations from the ANN model, were established. The developed regression equations were referred to as trained models. Then the predictive ability of the models was also tested with the same data sets employed for testing the ANN models. Therefore, the results are comparable.

The SRC model is carried out considering the following power law equation:

$$SSL = 6 \times 10^{-14} Q^{2.3496}. \tag{14}$$

5. Results and discussion

The prediction is performed by ANN, MLR, and SRC models for all input combinations and the results are presented in Table 4.

According to Table 4, the ANN and MLR models provided the best performance criteria for combination 5 and combination 3, respectively. In combination 5 (SSL_t, SSL_{t-1}, Q_t), the ANN structure was ANN

Table 4
R^2, MAE, and RMSE values in SSL prediction by ANN, MLR, and SRC models in the testing period.

Models	ANN						MLR						SRC
Combination	1	2	3	4	5	6	1	2	3	4	5	6	–
ANNs: Neurons in hidden layer	4	7	6	2	7	4	–	–	–	–	–	–	–
R^2	0.261	0.317	0.341	0.264	0.414	0.349	0.21	0.219	0.224	0.209	0.209	0.199	0.09
RMSE (ton/day)	6117.8	5880.8	5778.2	6107	5446.6	5743.9	6325.1	6289.4	6269.8	6331.6	6329.9	6371.2	6813.3
MAE (ton/day)	1526.2	1503.2	1452.8	1602.6	1414.8	1598.7	1948.5	2020.6	1985.2	1988.2	1654.3	1647.1	1736.2

Table 5
R^2, RMSE and MAE in SSL prediction by the WANN model in the testing period.

Mother wavelet type	Decomposition level	ANN structure	R^2	RMSE (ton/day)	MAE (ton/day)
Coif 1	1	4-1-1	0.744	3601.1	1149.6
Bior 1.1	3	8-2-1	0.527	4893.9	1167.3
Db 2	2	6-1-1	0.554	4751.8	1099.7
Meyer*	2	6-4-1	0.83	2935.1	898.3
Haar 1	2	6-4-1	0.632	4321	1021.7
Rbio 1.1	2	6-1-1	0.549	4779.3	1093.2
Sym 1	2	6-2-1	0.592	4548.8	1068

(3, 7, 1) representing 3, 7, and 1 input, hidden, and output neurons, respectively. The best MLR model used SSL_t, SSL_{t-1}, SSL_{t-2} as independent variables and SSL_{t+1} as dependent variable. In the ANN model, considerable improvements in the model performance was not found when the number of hidden neurons was increasing from a threshold, which is in accordance to the investigations reported by Abrahart and See (2000).

When multilevel sub-signals are entered in the WANN as input nodes, their assigned weights by the ANN method will be different at different decomposition levels; therefore, high weights will be applied to the high levels of the time series. For instance, in using order two for decomposition level, which yields three sub-signals for both Q and SSL time series, SSL_{t+1} is more relevant to $Q_{d2}(t)$ rather

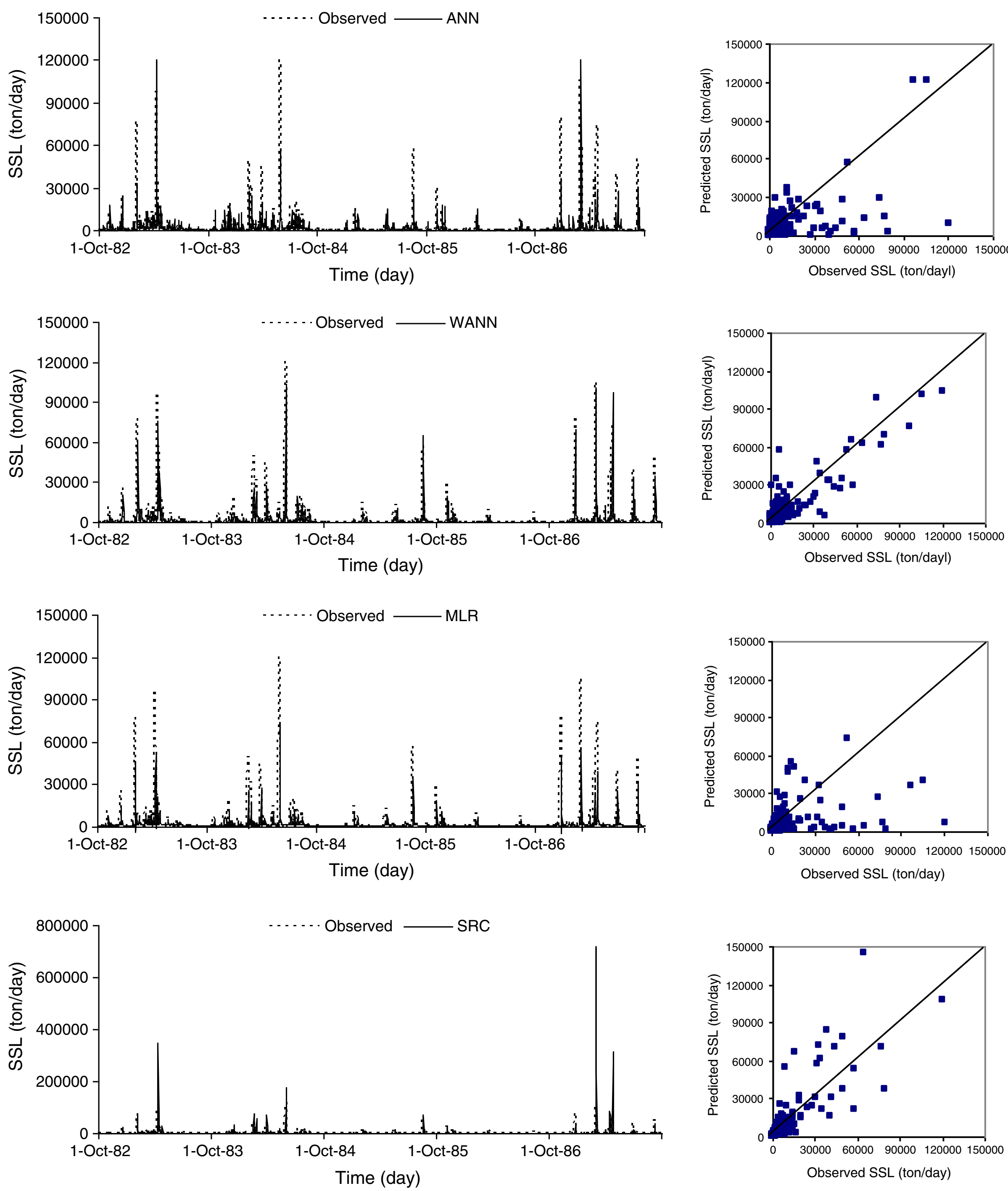

Fig. 6. Comparisons between the measured and predicted SSL based on the testing data.

than $Q_{d1}(t)$ because $Q_{d2}(t)$ (detail sub-signal of Q) is a short period in Q time series and has an important role in SSL prediction at time $t+1(SSL_{t+1})$. Therefore, the network magnifies its weight as comparatively as the other sub-signals.

In general, d_i can be substituted by different values. Considering direct relation among Q and SSL values, it is expected that both Q and SSL time series have the same seasonal levels. Therefore, decomposition levels for river discharge (Q_{di}) and SSL (SSL_{di}) time series have been considered equal. Obtained results by the WANN model, illustrated that by increasing the decomposition level, in levels greater than 2, the model performance is decreased because high decomposition levels lead to a large number of parameters with complex nonlinear relationships in the ANN approach. Although this relationship may monitor and fit the training data, each parameter creates an error in predicting data, consequently net errors decrease model performance. The level 2 can be considered as an appropriate decomposition level for the data but decomposition levels greater than two lead to low efficiency.

In the WANN model, long, intermediate, and short levels might be considered by selecting decomposition levels for Q and SSL time series. The proposed model not only pre-processes and partitions the SSL signal to effective calibrated time series, but also considers the influence of each sub-time series by magnifying its weight relatively. The performance of the WANN model is presented in Table 5.

In the structure of Meyer wavelet, Fig. 5d, which is similar to the SSL signal, the SSL signal features, especially its peaks could be considered. Consequently comparatively high performance is achieved. According to Tables 4 and 5, the R^2, MAE, and RMSE for the ANN model were in the ranges of 0.261 to 0.414, 1414.8 to 1602.6, and 5446.6 to 6117.8, respectively. The mentioned statistical parameters were in the ranges of 0.199 to 0.224, 1647.1 to 2020.6, and 6269.8 to 6371.2, respectively for the MLR model. For the SRC model, the mentioned parameters were 0.09, 1736.2, and 6813.3, respectively and the mentioned parameters were in the ranges of 0.527 to 0.83, 898.3 to 1167.3, and 2935.1 to 4893.9, respectively for the WANN model. The values of MAE and RMSE for WANN and ANN models were smaller than the values of these parameters for MLR and SRC models. Besides, R^2 for the intelligence models was more than R^2 for the conventional models.

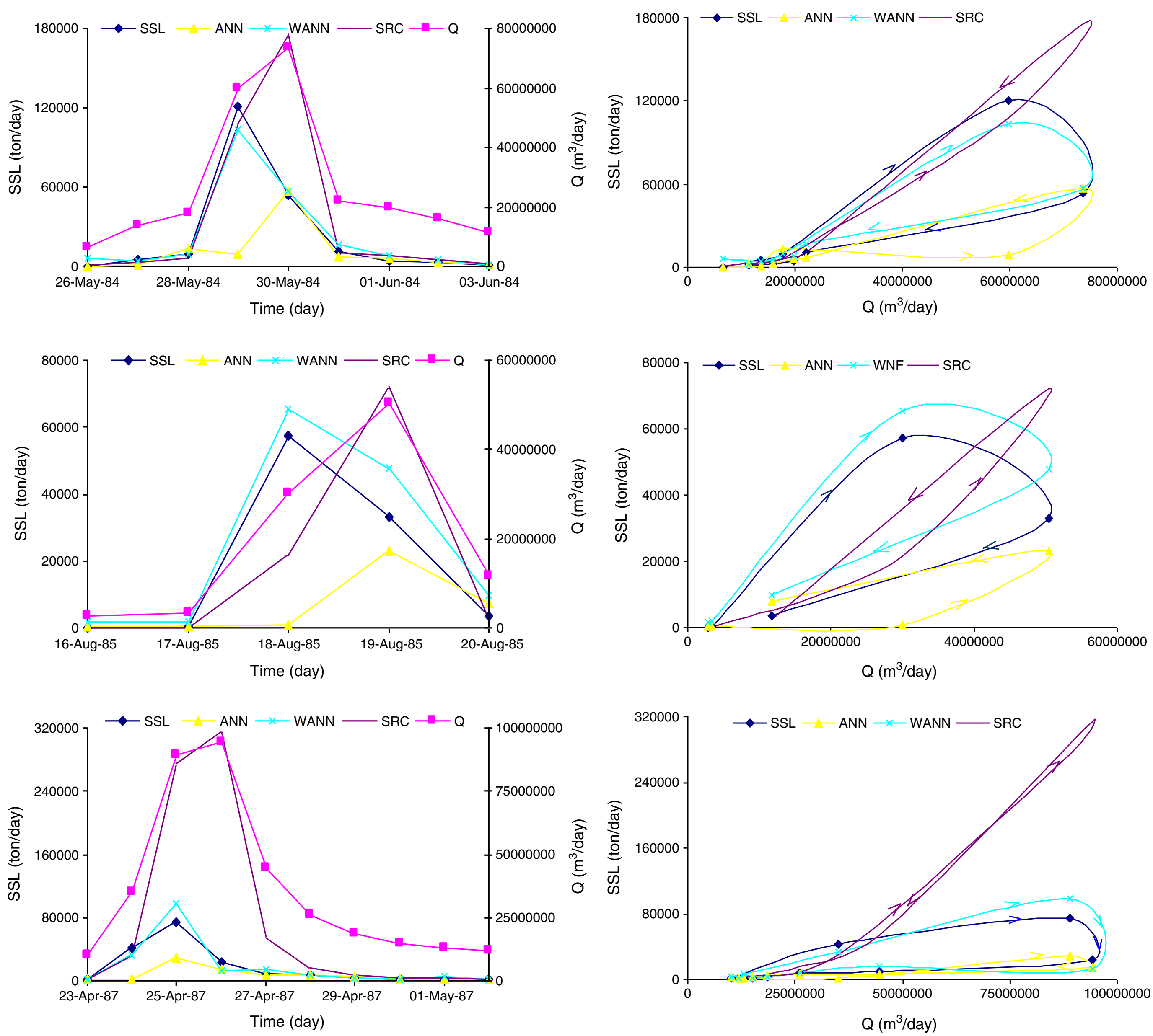

Fig. 7. Sediment graphs, hydrographs and hysteresis relations between Q and SSL of recorded storm events in the verification period.

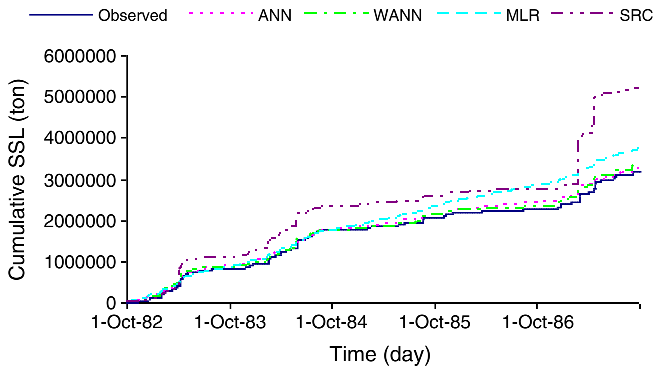

Fig. 8. Measured and estimated cumulative SSL in the testing period.

According to Tables 4 and 5, the best WANN model improved RMSE by 46.1%, 53.2%, and 84.4% in comparison to the best ANN, MLR, and SRC models, respectively. Because of employing the ANN technique for reconstruction of the time series, the proposed WANN model has a non-linear kernel; therefore, it can simulate the complex non-linear characteristics of the SSL phenomenon more accurately than the other linear models such as SRC and MLR. Results showed that the WANN model, which used decomposed data, had illustrated better performance than other models which employed row data. The SRC and MLR models consider linear regression among the variables; therefore, these approaches were not appropriate for handling the nonlinearity and complexity of the SSL phenomenon. Some modifications could be applied in order to increase the accuracy of the SRC method (e.g. using different fitted curves). Since just two calibrated parameters (i.e. a and b) were used, it was not expected that the outputs of the model could rival the artificial intelligence approaches results. In contrast to regression-based models, intelligence-based models use the advantage of multiple adjustable parameters and configurations; therefore, they are prone to problems of overfitting. Using time series plots, in Fig. 6, the predicted SSL values with the observed ones for testing period are compared.

As can be seen from Fig. 6, in the WANN model the SSL values were slightly underestimated during high SSL periods and fluctuated around the 1:1 line (in the scatter-plot) during low SSL periods. According to the scatter-plots, a comparison between WANN and other models obviously showed a significantly better performance of the former models. The discrete wavelet transform captures the dynamic properties of the nonlinear and non-stationary SSL time series using wavelet coefficients. The WANN is employed to include intelligent evaluation through a neural network model so as to extract useful features from discrete wavelet coefficients for obtaining effective components regarding SSL prediction. It could be seen that the wavelet analysis was extremely useful when it was used in SSL time series to extract important characteristics embedded in the SSL signal. The stated results indicated that the developed model could be an effective method in SSL prediction. In the following sections, several approaches such as hysteresis analysis, cumulative SSL estimation and prediction of high SSL values are used for evaluation of the models' performances.

5.1. Hysteresis analysis

Rivers are known to exhibit hysteresis in SSL (Horowitz, 2008), whereby SSL is greater on the rising limb of the hydrograph than on the falling limb. Besides the river sediment, the hysteresis event is noticed in other hydrologic processes too, for example, the soil moisture retention curve and the flood wave curve. Asselman (2000), Yang et al. (2007), and Jain (2008) mentioned the hysteresis in sediment process and presented the various models' performances in capturing this phenomenon.

Since the ANN and WANN models are powerful techniques for complex and nonlinear function mapping, this part deals with the application of these models to set up hysteresis phenomenon. The storms of May 26th, 1984, August 16th, 1985, and April 23rd, 1987 were selected for the hysteresis analysis in the testing period. The hydrographs, sediment graphs and rating loops of the selected storms are shown in Fig. 7. Moreover, the ANN, WANN, and SRC performances in simulation of hysteresis phenomenon are presented in Fig. 7.

According to Fig. 7, the peaks of SSL graphs precede the hydrograph peaks. The rating loops show hysteresis with a greater SSL for a given Q occurring on the rising limb rather than on the falling limb. Horowitz (2008) stated that the maximum SSL usually occurs prior to the peak Q. Clockwise (positive) hysteresis loops are observed for all storms, which strongly suggest that the progressive decline mechanism is dominant in sediment supply in the watershed. Clockwise trend of all floods is owing to the washout of fine loose material from in-channel erosion. A probable cause of positive hysteresis in the study area is depletion of available sediment before the peak of water discharge (e.g. Williams, 1989; Sayer et al., 2006).

The hysteresis simulations by the provided models were conducted to recognize rating loops using three storm events that occurred in the verification period. As seen in Fig. 7, the WANN model simulated the hysteresis event better than the other models. The ANN model simulated the hysteresis only in one event (i.e. April 23rd, 1987), while the SRC model was not able to simulate the hysteresis phenomenon. In the SRC method, SSL increased as a result of discharge's increase, which is due to the used power law between them. A major limitation of the SRC technique is that it was not able to take into account the hysteresis influence.

5.2. Cumulative SSL estimation

Sediment load computations are often the first step in river engineering and reservoir management. Also, the accurate estimation

Table 6
Evaluation of models in SSL prediction based on the testing period for values greater than 50,000 (ton/day).

Row	Date	Observed (ton/day)	ANN (ton/day)	WANN (ton/day)	MLR (ton/day)	SRC (ton/day)
1	29-May-84	120,598.9	8954.7	103,749.4	6158.4	107,515.3
2	02-Mar-87	105,796.8	120,598.9	101,167.6	39,206.5	717,523.4
3	11-Apr-83	97,511	120,598.8	76,230.1	35,764.3	348,607.2
4	25-Dec-86	79,814.6	2617.6	69,219.6	1655.4	37,628.5
5	03-Feb-83	77,500.8	15,096.9	61,584.7	6822.5	69,814.9
6	25-Apr-87	74,753.3	28,890.7	97,594.6	26,315.2	274,659.8
7	01-Mar-87	64,689.4	13,187.4	62,522.1	4389.8	144,649.8
8	10-Apr-83	57,723.8	2235.6	29,696.5	1986.3	52,667.1
9	18-Aug-85	57,428.4	704.9	65,508.9	1283.2	21,454.9
10	30-May-84	53,369.3	56,938.2	56,823.6	72,545.9	175,870.7
11	08-Sep-87	50,067.1	10,986.7	34,584.1	4222.1	37,031.2
R^2			−5.67	0.485	−7.82	−92.88
MAE (ton/day)			49,214.6	13,575	61,568.8	125,655.7
RMSE (ton/day)			56,939	15,819.1	65,476.3	213,652.4

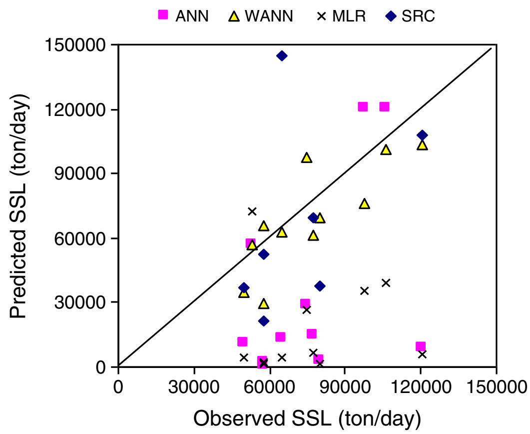

Fig. 9. Observed and predicted SSL in the testing period for SSL values greater than 50,000 (ton/day).

of sediment load is essential for the design and operation of dams, canals, and diversions. Since management decisions depend on sediment load computations, information about annual sediment load becomes a priority. In this study, the cumulative SSL was estimated 3.21, 3.32, 3.71, and 5.17 Mtonnes by ANN, WANN, MLR, and SRC models, respectively, while the measured value was 3.2 Mtonnes in the testing period. The ANN, WANN, MLR, and SRC models were overestimated by 0.5%, 3.9%, 16.02%, and 161.8%, respectively. The estimated cumulative SSL by the ANN and WANN models were closer to the observed data than the MLR and SRC models. Walling (1977) indicated that the annual sediment loads computed by employing a single SRC may involve overestimation by up to 60%. The SRC model considerably overestimated the cumulative SSL. The result is in accordance to the investigations reported by Walling (1977). Consequently, the SRC method cannot reasonably estimate the cumulative SSL. Measured and predicted cumulative SSL for the testing period are shown in Fig. 8.

5.3. Prediction of high SSL values

In this part of the study, prediction of high SSL values is performed by the models. The threshold for the SSL is taken as 50,000 (ton/day) and the results are presented in Table 6. The WANN model improved RMSE by 72.2%, 75.8%, and 92.6%, in comparison to the ANN, MLR, and SRC models, respectively.

Scatter plot of observed and predicted SSL obtained by all models for values greater than 50,000 (ton/day) is shown in Fig. 9. It was obvious that the WANN model prediction was closer to the 1:1 line than those predicted by the other models. The other models underestimated the SSL in all domains.

6. Summary and conclusion

An attempt was made in this paper to investigate the use of a hybrid WANN model for daily suspended sediment load prediction in Yadkin River at Yadkin College station in the USA. By utilizing an effective characteristic of wavelet analysis, i.e. discrete wavelet transform, with the concepts of neural networks, a new wavelet artificial neural network model was developed for SSL simulation in the river. In the provided model, the discharge and SSL signals were firstly decomposed into sub-signals with different scales, i.e. a large-scale sub-signal and several small-scale sub-signals in order to obtain temporal properties of the input time series. The decomposed SSL and Q time series were entered to the ANN method for prediction of SSL in one day ahead.

The comparison of the prediction accuracies of the WANN and other models indicated that the proposed WANN model could predict SSL time series because of using multi-scale time series of discharge and SSL data as the ANN input layer. Furthermore, the results showed that the proposed model could satisfactorily simulate hysteresis phenomenon, acceptably estimate cumulative SSL, and reasonably predict high SSL values. Thus wavelet and ANN combination model can be used as a useful approach for SSL time series modeling.

Data pre-processing method warrants further studies. It should be noted that generally in rivers, including Yadkin River, river discharge and SSL time series are characterized by high non-stationarity and non-linearity. ANN models may become unable to predict SSL due to these features, if pre-processing of the input and/or output data is not performed. Tests undertaken on preprocessed data, using a wavelet transformation, presented that the best results were obtained when the WANN model calibrated using a single ANN on the approximation coefficients at level two. In general, these results indicate a promising role of discrete wavelet transforms in SSL time series prediction.

In this research, a combined WANN intelligent model for prediction of SSL time series in rivers was proposed. Applying the methods developed in this study to the other phenomena requires more research. Using the presented approaches to predict the SSL in second, third or other following days and modeling SSL process by considering other variables (e.g. temperature or precipitation intensity) is suggested to improve the current study. Furthermore, as a plan for future studies, the presented methods can be used to simulate monthly and event based SSL time series.

References

Addison PS, Murrary KB, Watson JN. Wavelet transform analysis of open channel wake flows. J Eng Mech 2001;127(1):58–70.
Abrahart RJ, See L. Comparing neural network (NN) and Auto Regressive Moving Average (ARMA) techniques for the provision of continuous river flow forecasts in two contrasting catchments. Hydrol Process 2000;14:2157–72.
Alp M, Cigizoglu HK. Suspended sediment load simulation by two artificial neural network methods using hydro meteorological data. Environ Model Softw 2007;22: 2-13.
Altun H, Bilgil A, Fidan BC. Treatment of multi-dimensional data to enhance neural network estimators in regression problems. Expert Syst Appl 2007;32(2):599–605.
Asselman NEM. Fitting and interpretation of sediment rating curves. J Hydrol 2000;234: 228–48.
Bhattacharya B, Price R, Solomatine D. Data-driven modelling in the context of sediment transport. Phys Chem Earth 2005;30:297–302.
Cannas B, Fanni A, Sias G, Tronei S, Zedda MK. River flow forecasting using neural networks and wavelet analysis. EGU, European Geosciences Union, Vienna: Austria; 2005. p. 24–9.
Cannas B, Fanni A, See L, Sias G. Data preprocessing for river flow forecasting using neural networks: wavelet transforms and data partitioning. Phys Chem Earth 2006;31(18):1164–71.
Cohen A, Kovacevic J. Wavelets: the mathematical background. Proc IEEE 1996;84(4): 514–22.
Daubechies I. The wavelet transform, time–frequency localization and signal analysis. IEEE Trans Inf Theory 1990;36(5).
Engelund F, Hansen E. A monograph on sediment transport in alluvial streams. Copenhagen: Danish Technical; 1967 (Teknisk Forlag).
Fernando AK, Kerr T. Runoff forecasting with artificial neural network model. The 3rd Pacific Conference on stormwater and aquatic resource protection. Auckland: New Zealand Water and Wastes Association publication of conference proceedings in CD-ROM; 2003.
Gupta KK, Gupta R. Despeckle and geographical feature extraction in SAR images by wavelet transform. ISPRS J Photogramm 2007;62(6):473–84.
Haykin S. Neural network — a comprehensive foundation. Englewood Cliffs, NJ: Prentice-Hall; 1999.
Holtschlag DJ. Optimal estimation of suspended-sediment concentrations in streams. Hydrol Process 2001;15:1133–56.
Hornik K, Stinchcombe M, White H. Multilayer feedforward networks are universal approximators. Neural Netw 1989;2(5):359–66.
Horowitz AJ. An evaluation of sediment rating curves for estimating suspended sediment concentrations for subsequent flux calculations. Hydrol Process 2003;17: 3387–4009.
Horowitz AJ. Determining annual suspended sediment and sediment-associated trace element and nutrient fluxes. Sci Total Environ 2008;400:315–43.
Jain SK. Development of integrated discharge and sediment rating relation using a compound neural network. J Hydrol Eng 2008;13(3):124–31.
Kim TW, Valdes JB. Nonlinear model for drought forecasting based on a conjunction of wavelet transforms and neural networks. J Hydrol Eng 2003;8(6):319–28.
Kim B, Lee SE, Song MY, Choi JH, Ahn SM, Lee KS, et al. Implementation of artificial neural networks (ANNs) to analysis of inter-taxa communities of benthic microorganisms and macroinvertebrates in a polluted stream. Sci Total Environ 2008;390:262–74.

Kisi O. Suspended sediment estimation using neuro-fuzzy and neural network approaches. Hydrol Sci J 2005;50(4):683–96.
Labat D, Ababou R, Mangin A. Wavelet analysis in karstic hydrology 2nd part: rainfall-runoff cross-wavelet analysis, Comptes Rendus de l'Academie des Sciences Series IIA. Earth Planet Sci Lett 1999;329:881–7.
Labat D, Ababou R, Mangin A. Rainfall–runoff relation for karstic spring. Part 2: continuous wavelet and discrete orthogonal multi resolution analyses. J Hydrol 2000;238:149–78.
Legates DR, McCabe Jr GJ. Evaluating the use of goodness-of-fit measures in hydrologic and hydroclimatic model validation. Water Resour Res 1999;35(1):233–41.
Mallat SG. A theory for multi resolution signal decomposition: the wavelet representation. IEEE Trans Pattern Anal Mach Intell 1989;11(7):674–93.
Masters T. Practical neural network recipes in C++. San Diego (CA): Academic Press; 1993.
McCulloch WS, Pitts WH. A logical calculus of the ideas immanent in neural nets. Bull Math Biophys 1943;5:115–33.
Muller B, Reinhardt J, Strickland MT. Neural networks: an introduction. New York: Springer-Verlag; 1995. p. 52–62.
Nagy HM, Watanabe K, Hirano M. Prediction of load concentration in rivers using artificial neural network model. J Hydraul Eng 2002;128(6):588–95.
Osowski S, Garanty K. Forecasting of the daily meteorological pollution using wavelets and support vector machine. Eng Appl Artif Intell 2007;20:745–55.
Pasquini A, Depetris P. Discharge trends and flow dynamics of South American rivers draining the southern Atlantic seaboard: an overview. J Hydrol 2007;333:385–99.
Raghuwanshi N, Singh R, Reddy L. Runoff and sediment yield modeling using artificial neural networks: Upper Siwane River, India. J Hydrol Eng 2006;11(1):71–9.
Rajaee T, Mirbagheri SA, Zounemat-Kermani M, Nourani V. Daily suspended sediment concentration simulation using ANN and neuro-fuzzy models. Sci Total Environ 2009;407:4916–27.
Rajaee T. Wavelet and neuro-fuzzy conjunction approach for suspended sediment prediction. Clean-Soli, Air, Water 2010;38(3):275–86.
Raman H, Sunilkumar N. Multivariate modelling of water resources time series using artificial neural networks. Hydrol Sci J 1995;40(2):145–63.
Roberts G. The influence of sampling frequency on stream flow chemical loads. Water Environ J 1997;11(2):114–8.
Saco P, Kumar P. Coherent modes in multiscale variability of streamflow over the United States. Water Resour Res 2000;36:1049–68.
Sahoo GB, Ray C, Mehnert E, Keefer DA. Application of artificial neural networks to assess pesticide contamination in shallow groundwater. Sci Total Environ 2006;367:234–51.
Salas JD, Markus M, Tokar AS. Streamflow forecasting based on artificial neural networks. In: Rao G, Rao AR, editors. Chapter 4 in artificial neural networks in hydrology. London: Kluwer Academic Publishers; 2000. p. 23–51.
Sayer AM, Walsh RPD, Bidin K. Pipe flow suspended sediment dynamics and their contribution to stream sediment budgets in small rainforest catchments, Sabah, Malaysia. For Ecol Manage 2006;224:119–30.
Schmitz JE, Zemp RJ, Mendes MJ. Artificial neural networks for the solution of the phase stability problem. Fluid Phase Equilib 2006;245:83–7.
Snedecor GW, Cochran WG. Statistical methods. seventh ed. Iowa: Iowa State University Press; 1981.
Tantanee S, Patamatammakul S, Oki T, Sriboonlue V, Prempree T. Coupled wavelet-autoregressive model for annual rainfall prediction. J Environ Hydrol 2005;13 Paper 18.
Toffaleti FB. Definitive computations of sand discharge in rivers. J Hydraul Div ASCE 1969;95(1):1831–42.
Tokar AS, Johnson PA. Rainfall runoff modelling using artificial neural networks. J Hydrol Eng 1999;4(3):232–9.
Tsai CH, Chang LC, Chiang HC. Forecasting of ozone episode days by cost-sensitive neural network methods. Sci Total Environ 2009;407:2124–35.
Verstraeten G, Poesen J. Factors controlling sediment yield from small intensively cultivated catchments in a temperate humid climate. Geomorphology 2001;40:123–44.
Walling DE. Assessing the accuracy of suspended sediment rating curves for a small basin. Water Resour Res 1977;13(3):531–8.
Walling DE. Suspended sediment and solute response characteristics of the river Exe, Devon, England. In: Davidson-Arnott R, Nickling W, editors. Research in fluvial systems. Norwich: Geoabstracts; 1978. p. 169–97.
Ward P, Balen RT, Verstraeten G, Renssen H, Vandenberghe J. The impact of land use and climate change on late Holocene and future suspended sediment yield of the Meuse catchment. Geomorphology 2009;103:389–400.
Williams GP. Sediment concentration versus water discharge during single hydrologic events in rivers. J Hydrol 1989;111(1–4):89-106.
Yang G, Chen Z, Yu F, Wang Z, Zhao Y, Wang Z. Sediment rating parameters and their implications: Yangtze River, China. Geomorphology 2007;85:166–75.
Zhu YM, Lu XX, Zhou Y. Suspended sediment flux modeling with artificial neural network: an example of the Longchuanjiang River in the Upper Yangtze Catchment, China. Geomorphology 2007;84:111–25.
Zounemat-Kermani M, Beheshti AA, Ataie-Ashtiani B, Sabbagh-Yazdi SR. Estimation of current-induced scour depth around pile groups using neural network and adaptive neuro-fuzzy inference system. Appl Soft Comput 2009;9:746–55.